Magnetism of isolated cadmium atoms in vacancy-associated sites in nickel

W.-D. Zeitz
HMI Berlin, Bereich Strukturforschung, Glienicker Strasse 100, D-14109 Berlin, Germany
and School of Physical, Environmental and Mathematical Sciences, UNSW@ADFA, Canberra ACT 2600, Australia

R. Dogra
Department of Nuclear Physics, and Department of Electronic Materials Engineering, RSPhysSE, ANU, Canberra ACT 0200, Australia

A. P. Byrne
Department of Nuclear Physics, RSPhysSE, and Department of Physics, The Faculties, ANU, Canberra ACT 0200, Australia

S. K. Shrestha, A. V. J. Edge, and H. Timmers
School of Physical, Environmental and Mathematical Sciences, UNSW@ADFA, Canberra ACT 2600, Australia
(Received 26 September 2007; revised manuscript received 29 April 2008; published 3 July 2008)

The magnetic hyperfine fields of Cd guest atoms in nickel have been measured by perturbed angular correlation spectroscopy with an unprecedented precision. The experiments exhibit the well-known oscillations which have been attributed to the substitutional and the cubic *C*-site of Cd in nickel, but also show the existence of previously unknown sites through the observation of combined interactions between magnetic hyperfine fields and electric field gradients. The contributions of a large number of possible sites in connection with the properties of the combined interactions are proposed to be responsible for the invisibility of sites as well as for the large amplitudes of some measured frequencies. Following the systematic of magnetic fields of vacancy-associated 5sp-elements in nickel, the measured fields are consistent with theoretical expectations which use the number of vacancies as the primary parameter.

DOI: 10.1103/PhysRevB.78.014406 PACS number(s): 75.50.Cc, 31.30.Gs, 75.70.Rf

I. INTRODUCTION

From a large body of work, the magnetic hyperfine fields of vacancy-associated Cd sites in nickel are known to deviate from the value for the substitutional sites.[1–11] In previous publications, special attention was paid to the so-called "C-site," which develops in fcc metals during the annealing stage III. As no quadrupolar interaction was detected in these investigations, the *C*-site configuration was associated with a cubic environment. Originally the site was identified by the magnetic hyperfine field of $B_{\mathrm{hf}}(77\ \mathrm{K})=-2.80(5)$ T, but the interpretation was based on defect dynamics of vacancies. The corresponding magnetic field was allocated to a complex consisting of an interstitial Cd impurity surrounded by a tetrahedron of four vacancies.[1]

In follow-up experiments with other sp-elements, evidence was found for the existence of the same vacancy-associated configuration at Sn,[12–16] at In and at Te in nickel.[17,18] The Mossbauer measurements of ^{119}Sn in nickel also showed a manifold of sites with different numbers of vacancies being associated. Even larger vacancy complexes containing up to $n=100$ vacancies around Sn in nickel were discovered by positron annihilation experiments and became visible by optical methods.[19]

In contrast to this, the time-differential perturbed angular correlation (TDPAC) measurements of ^{111}Cd in nickel which were performed at the annealing stage III comply with the assumption of only three configurations and a fraction of unidentified sites called "missing fraction." Among these configurations there were two sites with cubic environment and one noncubic configuration which exhibited a magnetic hyperfine field of $B_{\mathrm{hf}}(\mathrm{RT})=-2.6(3)$ T and an electric field gradient of $V_{zz}=3\times10^{17}$ V/cm^2.[1,3,20] No trace of the single vacancy attached to Cd in nickel had been found, although this specific site should exist because the single vacancy site had been identified in many fcc metals by specific quadrupolar interactions.[21]

With the exemption of a few publications[10,20] the simultaneous presence of magnetic hyperfine fields and electric field gradients at Cd atoms in nickel have not caught sufficient attention in the past. In consequence, nearly no objection can be found in literature which challenged the interpretation of the most prominent oscillations in the perturbed angular correlation (PAC)-spectra. In most of these publications the detected oscillations were exclusively attributed to two cubic lattice sites, the substitutional site of Cd and the tetrahedral vacancy-associated site. The damping which was visible in most spectra was thought to be due to a distribution of magnetic fields.[22]

By the high-precision measurements of the current investigations, combined interaction spectra were obtained which require new ways of interpretation. As one experimental result, part of the "invisible fraction" of earlier measurements showed as "tails" in the lower frequency ranges adjacent to the prominent oscillations. After simulations of combined interaction spectra these tails are found to be composed from frequencies which are produced by a large variety of vacancy-associated Cd configurations. The second result came as a conflict to the allocation of the *C*-site to a cubic tetrahedral interstitial complex. Band-structure calculations propose that vanishing field gradients do not give notice of a cubic array of atoms or vacancies, because field gradients at

sp-element impurities are predominantly determined from the population of *p*-sublevels in the valence band.[23] As a second consequence, the large amplitude of the *C*-site configuration may be derived from the dynamic behavior of multi-vacancies or alternatively from a large number of possible vacancy complexes which have reasonably low-field gradients.

In an earlier publication de Waard *et al.*[18] have already proposed to correlate the magnitude of the magnetic hyperfine field at isolated sp-element atoms in nickel bulk with the number of vacancies around the impurity. Recent measurements have confirmed this correlation when using the coordination number, i.e., the number of nickel atoms that are adjacent to the guest atom, as the primary parameter for the interpretation of Cd surface sites on nickel.[24–28] The few *ab-initio* band-structure calculations which are available predict trends of magnetic hyperfine fields of sp-elements at surfaces[29–32] which agree with de Waard's conjecture for vacancy-associated bulk sites. According to the coordination-number dependence, the magnetic hyperfine field of $B_{\mathrm{hf}}=-2.8$ T at the Cd site in nickel matches the measured value of the $n=8$ and $n=7$ surface configurations. The coordination number $n=8$ is realized in a cubic vacancy-associated octahedral interstice and also in the substitutional site in nickel which is decorated with four vacancies.

In an early stage of the current investigations the results of the surface studies motivated us to resume measurements of the magnetic hyperfine fields for guest atoms in the nickel bulk. If the correlation between the number of vacancies and the magnetic hyperfine fields can be applied to complexes in the bulk, the distinction of vacancy-associated sites would be possible according to the magnitude of the magnetic field, for the first time. In addition, the ideas which have been outlined above call simple interpretations into question.

II. EXPERIMENTAL DETAILS

In these measurements, TDPAC spectroscopy using the radioisotope probe ^{111}In/^{111}Cd has been performed. Here the magnetic hyperfine fields for Cd in bulk nickel have been measured with better precision than done previously and the counts have been accumulated over a period long enough to discriminate between a beat pattern and damping. The probe ^{111}In/^{111}Cd was introduced into rolled high-purity nickel foils with two different ion implantation techniques. One foil was implanted with 125 keV $^{111}InO^{-}$ ions using the radioisotope implanter at UNSW@ADFA. A second foil was prepared by direct production and recoil implantation of the probe using the 14UD heavy ion accelerator at the ANU. A reference sample was also made by diffusing the radioisotope into a foil at 1000 °C followed by rapid quenching. Whereas the ion implantation techniques lead to defect complexes, the probes are known to adopt predominantly substitutional sites following sample preparation by diffusion and successive rapid quenching. The spectroscopy was carried out at room temperature (RT) and in some cases at 77 K with a setup of four BaF_2 detectors in standard 90°/180° TDPAC geometry.

The TDPAC method has been described elsewhere.[20,33,34] For the majority of the vacancy-associated sites of Cd in nickel, the $R(t)$-spectra of the TDPAC spectroscopy are expected to display the complexity which is characteristic of the combined interaction. Here the oscillation patterns depend on the ratio $y=\omega_L/\omega_0$ which is derived from the magnetic, ω_L, and the quadrupolar, ω_0, interaction frequencies. For each configuration, up to 15 frequencies and amplitudes have to be determined when using the $I=5/2$ isomeric level. As has been demonstrated earlier, TDPAC spectra for polycrystalline samples can hardly be measured if $\frac{1}{2}<y<2$.[20] If low electric field gradients are present, on the other hand, the Larmor frequencies will split and the splitting may be approximated by a distribution of frequencies.[35]

The Larmor frequency ω_L is related to the magnetic hyperfine field B_{hf} by $\omega_L=-g\,\mu_N B_{\mathrm{hf}}(T)/\hbar$. Here g is the nuclear g-factor of the isomeric level, $g=-0.3062(10)$,[36] and μ_N is the nuclear magneton. For polycrystalline samples the Larmor frequency can be determined by fitting the measured spectra to the time-dependent function $R(t)=A(a_1+a_2\cos\omega_L t+a_3\cos 2\omega_L t)$.[37] The amplitude A of this function is proportional to the fraction of probe nuclei on a specific site and the factors are $a_1=1/5$ and $a_2=a_3=2/5$, if the sample does not exhibit texture or is not subjected to a polarizing magnetic field. As long as cubic environments were expected for the substitutional and the *C*-site, the measured spectra were fitted to the above simple function. The quadrupolar interaction is based on the smallest observable interaction frequency $\omega_0=6e_oQV_{zz}/\hbar[4I(2I-1)]$ (half-integral spins I). Here the nuclear quadrupole moment for the $I=5/2$ nuclear level of ^{111}Cd is given by $Q=+0.83(12)b$.[38] The quantity V_{zz} stands for the largest diagonal tensor component of the traceless symmetric tensor. The other four components are the asymmetry parameter $\eta=(V_{xx}-V_{yy})/V_{zz}$ $(0\leq\eta\leq 1)$ and three Euler angles which determine the orientation of the diagonal tensor with respect to the fixed coordinate system. Together with three magnetic components, there are eight parameters to play a role in the combined interaction.

III. RESULTS AND DISCUSSION

In Fig. 1(a), one $R(t)$-spectrum is shown for the substitutional Cd site in Ni, which has been obtained after the sample had been rapidly quenched from the annealing temperature of 1000 °C. The fit was carried out assuming one occupied site exhibiting pure magnetic interaction with negligible damping. In contrast to this, the fits of the spectra in Figs. 1(b) and 1(c) delivered the two dominating Larmor frequencies that have been seen before in many investigations. Here a time-dependent damping of the amplitudes was introduced which was originally justified by a distribution of magnetic fields.[22]

The strongest frequency in the current spectra evident for the implanted samples, $\omega_{L,1}(77\ \mathrm{K})=104.6(1)$ Mrad/s and $\omega_{L,1}(\mathrm{RT})=97.8(1)$ Mrad/s, is in agreement with the field strength attributed to Cd on the substitutional site.[1,33,39] This assignment is confirmed as the frequency of $\omega_{L,1}(\mathrm{RT})=98.0(1)$ Mrad/s (with a fraction of 95% substitutional) is the only one found in the reference sample prepared by dif-

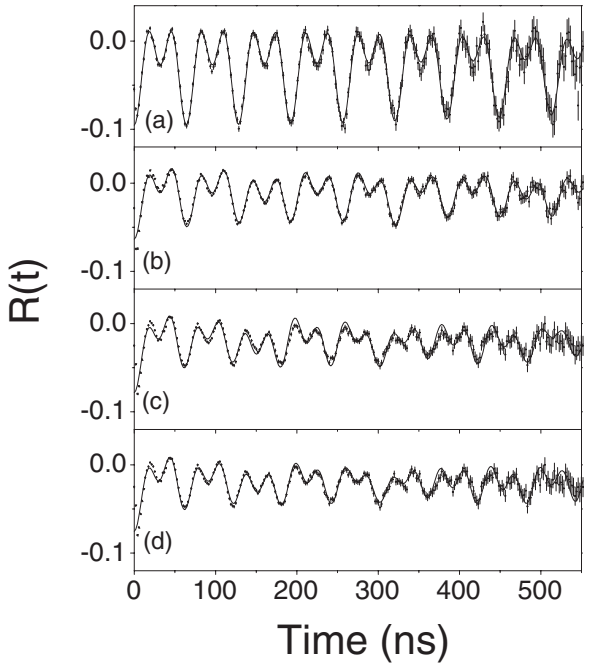

FIG. 1. PAC patterns measured in this work for ^{111}Cd in the nickel bulk and fits. (a) Measured at RT after the diffusion of the radioisotope at 1000 °C and rapid quenching. (b) Measured at RT following the 125 keV implantation of the probe. (c) Measured at 77 K after recoil implantation of the probe and fitted with only two frequencies $\omega_{L,1}$ and $\omega_{L,2}$. (d) The same as (c), but fitted with two frequencies $\omega_{L,1}$, $\omega_{L,2}$, and additional frequencies at ω_3=96.6(4) Mrad/s and ω_4=48.3(4) Mrad/s.

fusion at 1000 °C [Fig. 1(a)]. The very low damping points to a highly symmetric configuration, with only minor disturbances by irregularities in the lattice. After recoil implantation the substitutional fraction is only 47%. In the temperature range of interest, the magnetic fields for cubic sites follow the curve for the reduced spontaneous magnetization of nickel.[33] The hyperfine field is determined as $B_{\mathrm{hf}}(4.2\ \mathrm{K})=-7.11(3)$ T [1, 33, this work] using the nuclear g-factor $g=-0.306$. The association of this field with the substitutional site has been generally accepted, although band-structure calculations do not reproduce the field value. Lattice relaxation enhances the bond lengths around Cd impurities in Ni by about 3.5% and can change the absolute value of the field by 22% or 17%, depending on the "type of cell" used in the calculation, but is insufficient to explain the experimental value.[32,40] This failure has been related to the specific band structure of nickel,[40] since for impurities in iron and cobalt the inclusion of lattice relaxation is successful.[41,42] The substitutional site in the fcc lattice of nickel has a coordination number $n=12$.

Second in amplitude, the Larmor frequency $\omega_{L,2}(\mathrm{RT})=38.9(2)$ Mrad/s was measured following probe implantation with the radioisotope implanter which relates to a field magnitude of $|B_{\mathrm{hf}}(\mathrm{RT})|=2.65(2)$ T. The value of $\omega_{L,2}(77\ \mathrm{K})=41.6(2)$ Mrad/s was found after recoil implantation; see Figs. 1(b) and 1(c). The corresponding amplitudes indicate fractions of 14% and 26% of probes on this site, respectively. These magnetic fields correspond to the C-site which was originally associated with a magnetic hyperfine field of $B_{\mathrm{hf}}(\mathrm{RT})=-2.73(5)$ T.[1] Since the sign of the field cannot be determined from the new data, it has been adopted from that reference. The configuration for this field has been found to originate at an annealing temperature between 300 K and 650 K, which coincides with the temperature range of vacancy defect migration in the annealing stage III of metals.[1,9] The Cd impurity was suggested to occupy a tetrahedral interstitial site decorated by four vacancies.[1]

Similar frequencies had been found after different preparations, and especially the nature of the C-site defect has extensively been studied by nuclear techniques ranging from TDPAC, Mössbauer effect,[15] to NMR.[43] Using emission channeling measurements the existence of the tetrahedral interstice was confirmed.[44] The results of many investigations have been taken as support for the above allocations, but with the advent of the current measurements, experimentalists using the TDPAC technique have to pay sufficient attention to the peculiarities of the combined interaction before they can reduce the number of configurations they are discussing.

In particular, the above fits miss the beat patterns which are discernable in the measured high precision data. In a first attempt, two more frequencies at ω_3=96.6(4) Mrad/s and ω_4=48.3(4) Mrad/s were introduced to obtain the fit which is shown in Fig. 1(d). The amplitudes of these frequencies compare to an oscillation with a fraction of 9.8%, if a third cubic configuration was imagined to be present in the recoil-implanted sample. The fit complies with the most prominent beat of approximately 300 ns length but does not follow the "jumps" of the amplitudes which are clearly visible in the range before 300 ns. In order to improve the quality of the fits, we propose to allow sites other than cubic vacancy-associated sites to be included in the discussion.

The choice of adequate sites has to consider a very large number of possible configurations, according to the formula: $N(n,p)=n!/[(n\text{-}p)!p!]$. Focusing on regular sites in the fcc lattice of Ni the number of nearest neighbors, the coordination number, is $n=12$. One vacancy ($p=1$) will then have a choice between $N=12$ sites in the nearest shell, two vacancies ($p=2$) may organize in 66 different configurations, and $p=3$ in $N=220$, $p=4$ in $N=495$, $p=5$ in $N=792$ different configurations. Each of these configurations may exhibit its own set of 15 nonharmonic frequencies (for a nuclear spin of $I=5/2$).

The cubic tetrahedral and octahedral interstitial sites may also be decorated with vacancies. In contrast to the lighter elements such as carbon or fluorine the oversized Cd has no chance to occupy these interstitial sites in the fcc lattice of Ni directly, but will rather be in the center of vacancy-associated sites. The families of possible cubic sites in question for fcc lattices are listed in Table I. In row V_x the numbers of vacancies are given which are necessary to form the configurations. For rigid lattices, the relative distances to the atom in the center and the ratios of bond lengths are also given in Table I. The cubic C-site (T2) and the cubic vacancy-associated octahedral site (O2) are visualized in Fig. 2.

The coordination number n of an impurity in the bulk is derived by determining the number of occupied lattice points with equal distances to the impurity. For this purpose, one

TABLE I. Families of cubic vacancy-associated complexes for three sites in the nickel fcc lattice. Relative distances have been calculated from the center of the complex to the site of the neighboring atoms in the nonrelaxed lattice. The bond length of neighboring atoms in the undisturbed fcc lattice has the value of $\frac{1}{2}\sqrt{2}a$. The relative distances given in every fourth row refer to the n neighboring atoms after the removal of V_x lattice atoms in one or two shells, respectively.

Shell number	n	V_x	Relative distance to center	Ratio to bond length
Substitutional site, e.g., center at (0,0,0)				
S1	12	0	$\frac{1}{2}\sqrt{2}=0.707$	1
S2	6	12	$1=1.000$	1.414
S3	24	18	$\frac{1}{2}\sqrt{6}=1.225$	1.732
Tetrahedral interstitial site, e.g., center at $(\frac{1}{4},\frac{1}{4}),\frac{1}{4}$				
T1	4	0	$\frac{1}{4}\sqrt{3}=0.433$	0.612
T2	12	4	$\frac{1}{4}\sqrt{11}=0.829$	1.117
T3	12	16	$\frac{1}{4}\sqrt{19}=1.090$	1.541
Octahedral interstitial site, e.g., center at $(\frac{1}{2},0,0)$				
O1	6	0	$\frac{1}{2}=0.500$	0.707
O2	8	6	$\frac{1}{2}\sqrt{3}=0.866$	1.225
O3	24	14	$\frac{1}{2}\sqrt{5}=1.118$	1.581

lattice point is chosen to be the origin of a Cartesian coordinate system and vectors are assigned to each site in the cubic fcc lattice. Using the vector for the impurity at the center of the complex as reference, the distances to all lattice points in the vicinity of the impurity can be determined by vector analysis. When one complete shell of neighboring atoms is removed, the occupied lattice points in the next shell are counted. Using a hard-sphere configuration, the *C*-site complex, which is associated with four vacancies, has a cubic environment with $n=12$ neighboring Ni atoms in the nearest shell. In the fcc lattice of Ni, the coordination number $n=8$ is realized for a cubic octahedral interstice which is associated with six vacancies on positions in the face centers. Even bigger voids can be constructed by removing increasingly larger shells of neighboring atoms. The three possible families of vacancy-associated cubic complexes obtained this way are listed in Table I. We expect that the bigger cubic configuration will preferentially relax to noncubic agglomerates of vacancies around Cd.

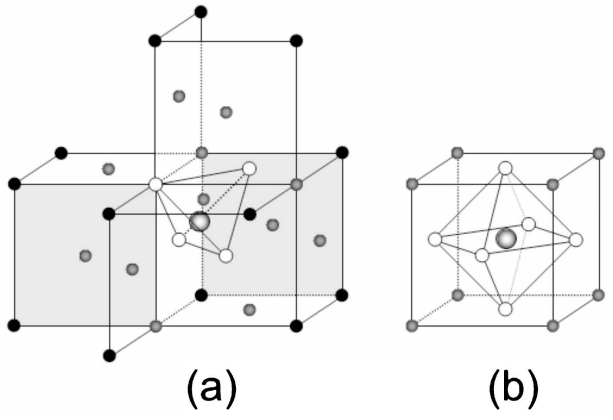

FIG. 2. Visualizations of vacancy-related Cd complexes in the nickel bulk. The nearest neighbors are indicated by gray spheres. (a) The cubic tetrahedral interstitial site of Cd in the fcc lattice of nickel. In this complex four nickel neighbor atoms of the Cd guest atom (large sphere) are replaced by vacancies (white spheres), $n=12$; (b) The octahedral interstitial site of Cd is surrounded by six vacancies, $n=8$.

On the basis of these considerations we calculated the number of possible vacancy-associated sites for the remaining cubic configurations. According to the above formula, we obtain the same numbers N of possible sites for the cubic vacancy-associated tetrahedral site as were found for the substitutional site. For the cubic octahedral site ($n=8$), the numbers p of vacancies correlate with N in the following way: $p=1\Rightarrow N=8$, $p=2\Rightarrow N=28$, $p=3\Rightarrow N=56$, $p=4\Rightarrow N=70$, $p=5\Rightarrow N=56$. As the total number of possible sites is very large, the identification of selected sites from the TDPAC spectrum is expected to be impossible, unless the manifold can be reduced.

First of all, quite a lot of these configurations are "filtered out" in the TDPAC method when $\frac{1}{2}<y=\omega_L/\omega_0<2$. This will be the case for classes of configurations which have the same electric field gradient but different directions of V_{zz}, if the magnetic hyperfine field satisfies the above condition. The mono-vacancy configuration attached at Cd in nickel is a good example. The magnetic interaction frequency in this configuration is expected to be close to the value on the substitutional site,[31] $\omega_L(\mathrm{RT})\approx 98$ Mrad/s, and the field gradient is estimated from the known value of Cd in Cu, $\omega_0\approx 109$ Mrad/s,[21] putting $y=0.9$ in the "unfavorable" range. The same argument was presented in an earlier publication on the basis of similar estimates.[10] In most spectra, the oscillation does not vanish completely from the spectrum, but 15 nonharmonic frequencies having comparable amplitudes deliver contributions to a weak oscillation pattern with no obvious periodicity. At the end we are confronted with the objection that a large number of frequencies which manifest various vacancy-associated sites is not likely to produce reasonable TDPAC spectra to identify specific configurations.

The existence of other sites, with y in a more favorable range, may be revealed by the "tails" which are clearly visible in the Fourier analysis in Fig. 3. Tails with similar shapes adjacent to dominant frequencies were discovered for ^{111}Cd at Co/Ag interfaces and were interpreted to stem from specific Cd sites at the interface which experience low-field gradients.[35] Following the same idea, the occupation of specific vacancy-associated sites is reflected in the spectra of the current investigations, if the field gradients are sufficiently low compared to the magnetic hyperfine fields and vice versa. But as long as scarce information is available about the magnitudes of the expected fields, the measured spectra cannot be allocated to specific configurations. The two dominant pairs of frequencies might be exempted from this perspective.

At last, two conflicting interpretations are possible to comply with the large amplitude of the *C*-site oscillation. One interpretation is based on models which estimate the

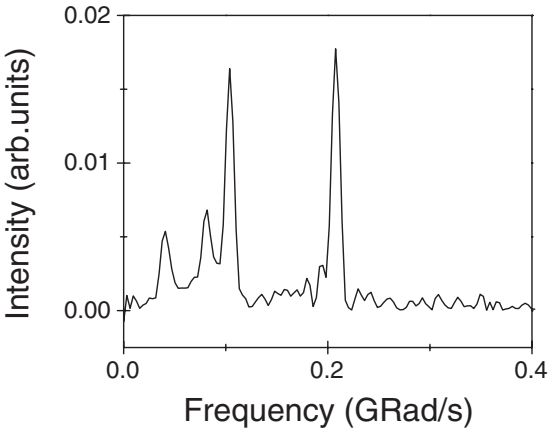

FIG. 3. Fourier analysis of the TDPAC spectrum of Cd in nickel after recoil implantation. The spectrum was measured at room temperature in an as-implanted sample.

mobility of interstitials, vacancies, and vacancy clusters at specific temperatures and deduce the development of the cubic *C*-site by proposing the capture of extremely mobile multi-vacancies at the Cd impurity.[4,8,10] Implicitly the model relies on an attractive interaction which drives the preferential formation of the complexes. The longer bond length in the *C*-site configuration when compared to the regular lattice site was estimated to be responsible for the reduced field strength.[22] This interpretation has been widely accepted in earlier publications and the magnetic hyperfine field of $B_{\mathrm{hf}}(\mathrm{RT})=-2.73(5)$ T (Ref. 1) has been used to identify the *C*-site configuration in nickel bulk after different preparation and annealing procedures.

The alternate interpretation, which is presented in this publication, is developed from the idea that a certain number of different vacancy distributions which may be present around the Cd impurities may deliver contributions to produce the large amplitude which is seen at some frequencies in the measured spectrum. Here the interpretation of the spectrum lives from the expectation that a substantial fraction of configurations with low-field gradients and magnetic hyperfine field close to measured value can be expected to be among the 495, or 792 and even more possible configurations.

In general, low-field gradients are expected to be present in atomic arrangements which are close to ideal cubic symmetries. But following $V_{zz}\approx\Delta n_p=\frac{1}{2}(n_{px}+n_{py})-n_{pz}$ for cylindrical charge distributions, low-field gradients may also exist at sp-elements with nearly balanced occupations n_{pi} in the *p*-subshells.[23] The field gradients at Cd adatoms on Ni (100) and Ni (111) surfaces, e.g., support this concept.[28] Taking the above finding into account, a sufficiently large number of configurations is likely to be found among associations with four or five vacancies. The results of the calculations also limit the applicability of the point charge model to exceptional cases and put interpretations at risk if the existence of cubic configurations is exclusively derived from vanishing field gradients.

Before obtaining the fits which are depicted in Fig. 1, various combined interactions had been supplemented. A reasonable result was achieved using a field gradient of $V_{zz}\approx 0.15\times 10^{17}$ V/cm^2 or, equivalently, a damping constant of $\lambda=3.5$ MHz. Preceding NMR measurements on In in nickel were insensitive to field gradients lower than $V_{zz}\approx 10^{17}$ V/cm^2.[43]

Reliable estimates for magnetic hyperfine fields at the vacancy-associated Cd sites in nickel bulk are also necessary to be obtained. In accordance with the coordination-number dependence, which was originally found to work for sp-elements at surface sites, identical magnetic fields are assumed for configurations which are associated with equal numbers of vacancies. Realizing that the value of the magnetic hyperfine field, $B_{\mathrm{hf}}(\mathrm{RT})=-2.65(2)$ T, which was measured in the bulk, is close to the value measured for the $n=8$ and the $n=7$ Cd surface sites on nickel,[24,25] we propose to confine the discussion to complexes with four or five vacancies. Here it shall be left open whether a substantial contribution to the measured amplitudes of the *C*-site configuration may stem from the cubic tetrahedral interstice.

In theoretical approaches the magnetic hyperfine fields are estimated with the help of models which describe the behavior of sp-elements by the dominating influence of the Fermi contact interaction of *s*-conduction electrons.[40–42,45] In these calculations the magnetic fields are derived from the local level density structure of scattered conduction *s*-electrons[29–32] and changes in symmetry are found to have only small effects.[27] The model reproduces the measured trends of magnetic fields, although lattice relaxations are not considered.[28] In the discussions we adopted magnetic fields from measurements for Cd on nickel surfaces[26] and recent calculations for 5sp-element impurities.[31] The respective coordination numbers are inversely proportional to the numbers of vacancies at regular lattice sites. Bellini *et al.*[32] have calculated a reduction of the magnetic field by 43% in the hypothetical bcc-nickel ($n=8$) relative to that for $n=12$ bulk configurations. The same authors find similar field reductions for some noncubic substitutional sites which are decorated by four vacancies, if they use the same "cell-type," regardless of the symmetry.

Summarizing the above discussion we point out that one specific configuration may not be enough to be attributed to the hyperfine parameters which were measured for the *C*-site. Further insight is hampered by the fact that no calculations are available for a sufficient number of vacancy-associated sites in the bulk. The concept of the coordination-number dependence is proposed to be applied, as a first step, in order to identify configurations of sp-elements in imperfect bulk lattices in analogy to the accepted surface theory. A generalization to other 5sp-elements should be possible, since model calculations show similarities in the local *s*-wave level densities for these elements. A reanalysis of published data for the elements Sn, Sb, and Te in nickel[12–18] is likely to give support to the concept. At this point the discussion in this paper merges with an earlier proposition of de Waard *et al.* who attributed the *C*-site configurations of Sn, Sb, and Te in nickel to agglomerates of four vacancies around these elements.[18] At that time, the theory of Blandin and Campbell[46] failed to follow the measured trend of magnetic hyperfine fields, but recent theories using the real-space Green's function embedding method[31] are much closer to the experimentally determined systematic. In Fig. 4, the theoret-

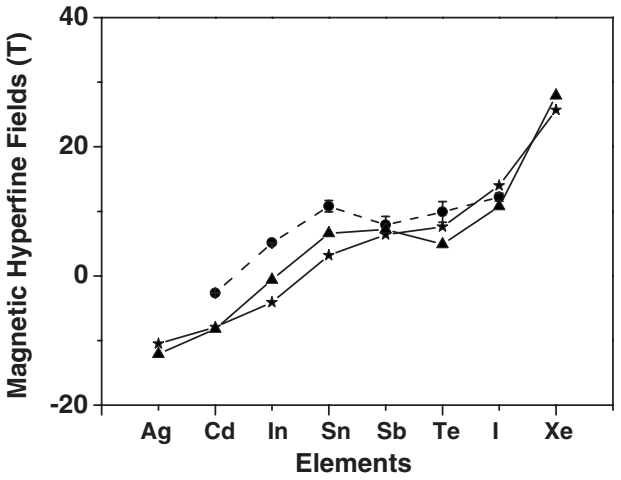

FIG. 4. Measured magnetic hyperfine fields of 5sp-elements in nickel bulk compared to calculations for fields at nickel surface sites. The configurations with the coordination numbers $n=7$ (triangles) and $n=8$ (stars) are selected from the calculations for surface sites (Ref. 31). The numbers of vacancies at substitutional sites are $N_v=12-n$. The experimental values for vacancy-associated sites (dots) at Cd are taken from this work, at In from Refs. 17 and 43, and for Sn, Sb, Te and I from Ref. 18.

ical results, which have originally been calculated for the $n=8$ and $n=7$ nickel surface sites,[31] are compared with the experimentally determined fields at vacancy-associated sites of Cd in nickel [this work], of In in nickel,[17,43] and with the values which are given for the other elements in de Waard's paper.[18] The expected fields which are estimated for other coordination numbers deviate significantly from the fields for the $n=8$ and $n=7$ clusters. Ignoring the problem of most theories to predict the absolute values of the magnetic hyperfine fields in nickel bulk, the measured trend in the magnetic fields across the period of elements is satisfactorily reproduced by the predictions for sites which are associated with four or/and five vacancies.

ACKNOWLEDGMENTS

The authors acknowledge the staff of the School of Physical, Environmental and Mathematical Science of UNSW&ADFA and of the ANU Heavy-ion Facility for their assistance in this work. One of us gratefully remembers the hospitality and the support during his time as a visitor to UNSW&ADFA.

[1] C. Hohenemser, A. R. Arends, H. de Waard, H. G. Devare, F. Pleiter, and S. A. Drentje, Hyperfine Interact. **3**, 297 (1977).
[2] R. M. Suter, M. Haoui, and C. Hohenemser, Hyperfine Interact. **4**, 711 (1978).
[3] F. Pleiter, Hyperfine Interact. **5**, 109 (1977).
[4] G. S. Collins and R. B. Schuhmann, Hyperfine Interact. **15**, 391 (1983).
[5] J. R. Fransens, F. Pleiter, and J. M. Meinders, Hyperfine Interact. **60**, 743 (1990).
[6] G. S. Collins and R. B. Schuhmann, Phys. Rev. B **34**, 502 (1986).
[7] J. R. Fransens, F. Pleiter, and J. M. Meinders, Solid State Commun. **71**, 1155 (1989).
[8] G. S. Collins, S. L. Shropshire, and J. Fan, Hyperfine Interact. **62**, 1 (1990).
[9] L. Chow and X. Zhao, Hyperfine Interact. **78**, 563 (1993).
[10] C. Allard, G. S. Collins, and C. Hohenemser, Phys. Rev. B **32**, 4839 (1985).
[11] C. Allard, G. S. Collins, and C. Hohenemser, Hyperfine Interact. **15–16**, 387 (1983).
[12] H. deWaard, D. W. Hafemeister, L. Niesen, and F. Pleiter, Phys. Rev. B **24**, 1274 (1981).
[13] G. Weyer, F. T. Pedersen, H. Grann, and K. Bonde-Nielsen, Hyperfine Interact. **29**, 1233 (1986).
[14] E. Danielsen, K. B. Nielsen, J. W. Petersen, M. Søndergaard, and G. Weyer, Mater. Sci. Forum **15-18**, 669 (1987).
[15] K. Bonde-Nielsen, E. Danielsen, J. W. Petersen, M. Søndergaard, and G. Weyer, Hyperfine Interact. **35**, 643 (1987).
[16] H. de Waard, Hyperfine Interact. **40**, 31 (1988).
[17] L. Niesen, Hyperfine Interact. **79**, 701 (1993).
[18] H. de Waard, G. L. Zhang, and R. H. Huizenga, Hyperfine Interact. **52**, 229 (1989).
[19] G. Dlubek, O. Brümmer, N. Meyendorf, P. Hautojärvi, A. Vehanen, and J. Yli-Kauppila, J. Phys. F: Met. Phys. **9**, 1961 (1979).
[20] F. Pleiter, A. R. Arends, and H. G. Devare, Hyperfine Interact. **3**, 87 (1977).
[21] F. Pleiter and C. Hohenemser, Phys. Rev. B **25**, 106 (1982).
[22] F. Raether, G. Weyer, K. P. Lieb, and J. Chevallier, Phys. Lett. A **131**, 471 (1988).
[23] S. Cottenier, V. Bellini, M. Çakmak, F. Manghi, and M. Rots, Phys. Rev. B **70**, 155418 (2004).
[24] H. Granzer, H. H. Bertschat, H. Haas, W.-D. Zeitz, J. Lohmüller, and G. Schatz, Phys. Rev. Lett. **77**, 4261 (1996).
[25] K. Potzger, A. Weber, H. H. Bertschat, W.-D. Zeitz, and M. Dietrich, Phys. Rev. Lett. **88**, 247201 (2002).
[26] K. Potzger, A. Weber, W.-D. Zeitz, H. H. Bertschat, and M. Dietrich, Phys. Rev. B **72**, 054435 (2005).
[27] M. J. Prandolini, Y. Manzhur, A. Weber, K. Potzger, H. H. Bertschat, H. Ueno, H. Migoshi, and M. Dietrich, Appl. Phys. Lett. **85**, 76 (2004).
[28] Y. Manzhur, W.-D. Zeitz, M. J. Prandolini, W. D. Brewer, P. Imielski, J. Schubert, K. Johnston and the ISOLDE-Collaboration, Eur. Phys. J. B **59**, 277 (2007).
[29] Ph. Mavropoulos, N. Stefanou, B. Nonas, R. Zeller, and P. H. Dederichs, Phys. Rev. Lett. **81**, 1505 (1998).
[30] Ph. Mavropoulos, N. Stefanou, B. Nonas, R. Zeller, and P. H. Dederichs, Philos. Mag. B **78**, 435 (1998).
[31] Ph. Mavropoulos, J. Phys.: Condens. Matter **15**, 8115 (2003).
[32] V. Bellini, S. Cottenier, M. Çakmak, F. Manghi, and M. Rots, Phys. Rev. B **70**, 155419 (2004).
[33] D. A. Shirley, S. S. Rosenblum, and E. Matthias, Phys. Rev.

170, 363 (1968).
[34] V. Samohvalov, Ph.D. thesis, Technische Universität Bergakademie Freiberg, 2003.
[35] M. Neubauer, K. P. Lieb, P. Schaaf, and M. Uhrmacher, Phys. Rev. B **53**, 10237 (1996).
[36] R. B. Firestone and V. S. Shirley, *Table of Isotopes*, 8th ed. (Wiley, New York, 1996).
[37] E. Matthias, S. S. Rosenblum, and D. A. Shirley, Phys. Rev. Lett. **14**, 46 (1965).
[38] P. Herzog, K. Freitag, M. Reuschenbach, and H. Walitzki, Z. Phys. A **294**, 13 (1980).
[39] G. N. Rao, Hyperfine Interact. **24–26**, 1119 (1985).
[40] H. Haas, Hyperfine Interact. **151–152**, 173 (2003).
[41] S. Cottenier and H. Haas, Phys. Rev. B **62**, 461 (2000).
[42] T. Korhonen, A. Settels, N. Papanikolaou, R. Zeller, and P. H. Dederichs, Phys. Rev. B **62**, 452 (2000).
[43] A. Metz and L. Niesen, J. Phys.: Condens. Matter **2**, 1705 (1990).
[44] L. M. Howe, M. L. Swanson, and A. F. Quenneville, Nucl. Instrum. Methods Phys. Res. **218**, 663 (1983).
[45] H. Katayama-Yoshida, K. Terakura, and J. Kanamori, J. Phys. Soc. Jpn. **48**, 1504 (1980).
[46] A. Blandin and I. A. Campbell, Phys. Rev. Lett. **31**, 51 (1973).